Polymer 181 (2019) 121764

Contents lists available at ScienceDirect

Polymer

journal homepage: www.elsevier.com/locate/polymer

Does the nature of chemically grafted polymer onto PVDF decide the extent of electroactive β-polymorph?

Amanuel Gebrekrstos[a], Goutam Prasanna Kar[b], Giridhar Madras[a,c], Ashok Misra[c], Suryasarathi Bose[b,*]

[a] Department of Chemical Engineering, Bangalore, 560012, India
[b] Department of Materials Engineering, Bangalore, 560012, India
[c] Interdisciplinary Center for Energy Research, Indian Institute of Science, Bangalore, 560012, India

HIGHLIGHTS

- One-pot modification of PVDF via ozonization process was attempted.
- PVDF with crystalline-amorphous and crystalline-crystalline grafts were synthesized.
- The polar β phase increased from 38% in untreated PVDF to 84% after ozonization.
- Interestingly, by grafting a crystalline polymer onto PVDF near-complete transformation from α to β phase was observed.
- β enhanced grafted polymers had higher dielectric constant and piezoelectric coefficient as compared to untreated PVDF.

ARTICLE INFO

Keywords:
Ozone treated PVDF
β-phase
Dielectric properties
Piezoelectric coefficient
PVDF copolymers

ABSTRACT

PVDF, one of the most versatile fluoropolymers, is inert and is difficult to functionalize using conventional approaches. Herein, we attempted a facile and one-pot modification of PVDF via ozonization process. The ozone treated PVDF facilitates in harnessing suitable functional moieties. Using this strategy, two copolymers were designed to achieve crystalline-amorphous and crystalline-crystalline grafts. Their effects on phase transformation, dielectric and piezoelectric behaviors of PVDF were systematically investigated. The microstructure and phase transformation of this modified PVDF copolymer was characterized by XPS, XRD, FTIR, SAXS, and DSC. FTIR results revealed that the extent of polar β phase increased from 38% in untreated PVDF to 84% after ozonization. Interestingly, the enhancement is more pronounced after grafting. For instance, after grafting a crystalline polymer, poly (butylene succinate-co-adipate) (PBSA) onto PVDF near-complete transformation from α to β phase (96%) was observed. This was attributed to the specific covalent interaction between the –OH group in PVDF-OH and –COOH groups of PBSA. This strong covalent interaction helps to align the PVDF chains in trans conformation and as a result more β phase crystals are formed. The long period (L_w) calculated from SAXS for an amorphous graft as in PVDF-g-poly(methyl methacrylate-co-acrylic acid) (PMM-co-AA) and PVDF-g-PBSA decreased significantly as compared to neat PVDF. The remarkably enhanced β phase in the grafted polymers reflected in higher dielectric constant and piezoelectric coefficient (d_{33}) as compared to untreated PVDF. For instance, the PVDF-g-PBSA copolymer showed higher piezoelectric and dielectric constant with low dielectric loss as compared to untreated PVDF. This study attempts to address whether the nature of graft (crystalline vs amorphous) decides the extent of β-PVDF and piezoelectric properties in PVDF copolymers.

1. Introduction

To meet the ever-increasing demand of dielectric materials in electronic industries, materials with high piezoelectric coefficient are required for energy storage devices [1]. Among the dielectric materials, ceramics, polymers, and polymer composites are widely used. Although ferroelectric ceramics such as $Pb(Zr,Ti)O_3$ (PZT), $Pb(Mg_{0.33}Nb_{0.77})O_3$-$PbTiO_3$ (PMNT) and $BaTiO_3$ (BT) with very high dielectric constant are available to meet most of the demands but they are brittle and possess low dielectric strength [2]. On the other hand, piezoelectric polymers

* Corresponding author.
E-mail address: sbose@iisc.ac.in (S. Bose).

https://doi.org/10.1016/j.polymer.2019.121764
Received 10 May 2019; Received in revised form 17 August 2019; Accepted 30 August 2019
Available online 05 September 2019
0032-3861/

such as PVDF, nylon 11, PU, and TPU have very low dielectric constant and very high breakdown strength [3,4]. Among the piezoelectric polymers, PVDF shows outstanding piezoelectric properties and are widely used in sensors, actuators, and energy storing devices [4–6]. The piezoelectric applications in PVDF stem from the existence of different crystalline phases, namely, α, β, γ and δ [7]. The α phase is non-polar and dielectrically less active as compared to others. The β and γ phases are polar and are well known for its excellent piezoelectric and pyroelectric properties [8,9]. Due to this a large number of strategies have been established to obtain electro-active β phase in PVDF. The most common ways to obtain polar β phase include rolling [10], stretching [11,12], shearing [13], casting from solution, poling, quenching from melt [14], etc. It is reported that by blending PMMA, PET, and PVC at low concentration also results in β-PVDF in the blends [15]. For example, blending PVDF with fewer concentrations of PMMA favors β phase formation in PVDF [16]. The addition of PMMA results in higher glass transition of PVDF in the blends thereby facilitates β phase formation. Though all the strategies resulted in β phase formation, their orientation in the preferred direction decides the end application.

Recently, incorporation of fillers such as $CoFe_2O_4$ nanoparticles [17], MWNTs [18], GO/RGO [19], have proven to be an efficient strategy to obtain polar β phase and enhanced piezoelectric properties in PVDF nanocomposites. Among all carbonaceous fillers such as GO and CNTs have received much attention due to its high aspect ratio, mechanical, thermal, and electrical properties. For example, Costa et al. reported that mechanical stretching is an effective strategy to induce β-PVDF in PVDF/CNF composites [20]. Further, high dielectric permittivity was observed due to the formation of β phase as compared to neat homopolymer. Huang et al. also reported that incorporation of high aspect ratio CNTs exhibited a noticeable influence on the formation of β phase as compared to low aspect ratio CNTs [21].Yu et al. also explained the formation of β after incorporation of CNTs in PVDF by solution sonication method [22]. The confinement created by TT-type molecular chain acts as a nucleating agent thereby resulting in β phase formation. Though CNTs facilitate β phase formation, dispersion in the matrix still remains an open challenge in this area. Graphene derivatives have attracted considerable scientific interest in recent years. This is due to the polar functional group such as C═O, O-H, C-O-C on the GO plane that can promote attractive interaction with the polymer matrix [23]. Achaby et al. demonstrated that the incorporation of graphene oxide nanosheets (GOn) into PVDF resulted in the formation of electroactive β phase [24]. The strong interactions between the CF_2 group of PVDF and C═O groups in GOn are responsible for the formation of pure β phase. Layek et al. [25] also reported that the incorporation of PMMA modified graphene nanosheets induces polar β phase. The dipole attraction between > CF_2 of PVDF and > C═O of the grafted PMMA and orientation of GO are responsible for the TTTT conformation. It was also reported that addition of TiO_2–GO into PVDF promotes β phase formation [26]. Enhaced amount of β-phase and dielectric properties were observed for PVDF/MG@GO7.0 composite [27]. Fluorine-doped graphene oxide also induced β phase and high energy density due to polarization center rendered by fluorine [28].

The orientation and amount of β phase present in PVDF determines the piezoelectric coefficient, dielectric permittivity, and energy density. For example, Mohammadi et al. investigated the effect of drawing temperature and stretching ratio on the content of β phase and piezoelectric coefficient [29]. Samples with high β phase showed higher piezoelectric coefficient ca. 33 pC/N after stretching followed by poling. Gomes et al. also showed that stretching of PVDF thin films at 87 °C and 6.5 stretching ratios, produced maximum β phase and enhanced piezoelectric coefficient as compared to control samples [30,29]. Kaura et al. also reported that maximum piezoelectric constant (60 pC/N) in PVDF by stretching followed by poling [31]. Apart from the polymer/filler composites, copolymers of PVDF such as PVDF-HFP [32], PVDF-TrFE-CFE [33], PVDF-TrFE [34] have also attracted attention as potential piezoelectric materials [35]. Although fluoropolymers have many applications in electronic industries, the lack of functional groups on their main chain limits their application. To overcome this, several modification routes such as ozonization [36], plasma treatment [37] and electron beam (EB) exposure [38] have been reported to incorporate desirable functionalities. For example, Ying et al. indicated ozone treated PVDF copolymerized with Poly(acrylic acid) (AAc-g-PVDF) for membrane application [39]. Dong et al. also showed ozone treated PVDF, PVDF-g-PBPMA for UV absorbing membranes [40]. In general, most of the works on ozone treated PVDF are to incorporate functionalities for membrane applications but the effect of this strategy on β formation and the piezoelectric response received less attention. In this study, PVDF-OH has been prepared via ozonization and used to graft PMM-co-AA and PBSA polymers. The –OH groups on PVDF-OH react with –COOH group present in PMM-co-AA and PBSA to form an ester. The effects of functionalization and further grafting on the polar β phase formation and piezoelectric coefficient in PVDF have been investigated.

2. Experimental section

2.1. Materials

Powder PVDF ((Kynar-761 with Mw of 440, 000 g/mol) was obtained from Arkema Inc. PBSA (Bionolle 3001MD with M_w 240,000 g/mol) was gifted by SHOWA DENKO K.K Japan. N,N-dimethylformaide (DMF) was used as a solvent and obtained from Aldrich Chemical Co.

2.2. Sample preparations

3 g of powder PVDF was dissolved in 50 ml of DMF for 1 h under mechanical stirrer. The solution was placed in 250 ml two-necked round bottom flask. A mixture of O_3/O_2 (generated from ozone generator) was continuously bubbled through the solution at a flow rate of 60 l/h at 25 °C for 8 h under nitrogen atmosphere. After the ozone treatment, the polymer solution was poured into glass petri-dish and dried at room temperature.

2.3. Synthesis of PVDF-g-PMM-co-AA and PVDF-g-PBSA

About 3 g of PVDF-OH and 3 g of PMM-co-AA was dissolved in 50 ml of DMF. Then a solution of 0.2 g DCC and 0.1 g DMAP in DMF were added. The solution was introduced into a 2 necked flask and was placed in an oil bath followed by stirring at 80 °C for 7 h. Finally, the solution was poured into a glass petri-dish and dried at room temperature. Similarly, PBSA was grafted onto PVDF. The processes of ozonization of PVDF and further grafting of PMM-co-AA and PBSA are represented schematically in Fig. 1a and b respectively.

2.4. Thin film fabrication

Thin films of PVDF-OH, PVDF-g-PMM-co-AA, and PVDF-g-PBSA were fabricated by two methods (i) by casting the graft copolymer solution onto a glass petri dish and dried at 60 °C (ii) by hot pressing at 220 °C under a pressure of 10 bar for 5 min. The thickness of the copolymers was ca. 120 μm and were used for dielectric measurements.

2.5. Characterizations

The functionalization of powder PVDF and the presence of different phases were analyzed by FTIR. FTIR spectra of powder (untreated) PVDF, ozone treated PVDF, PVDF-g-PMM-co-AA, and PVDF-g-PBSA was carried out in the range of 4000 to 650 cm^{-1} with a resolution of 4 cm^{-1}. The XRD was performed using Cu Kα radiation (40 KV) at a scan rate of 0.04° s^{-1} in the range of 10 to 60° range of 2θ to determine the different crystalline structure of neat and ozone treated PVDF. The X-ray photoelectron spectroscopy (XPS) measurements were carried out

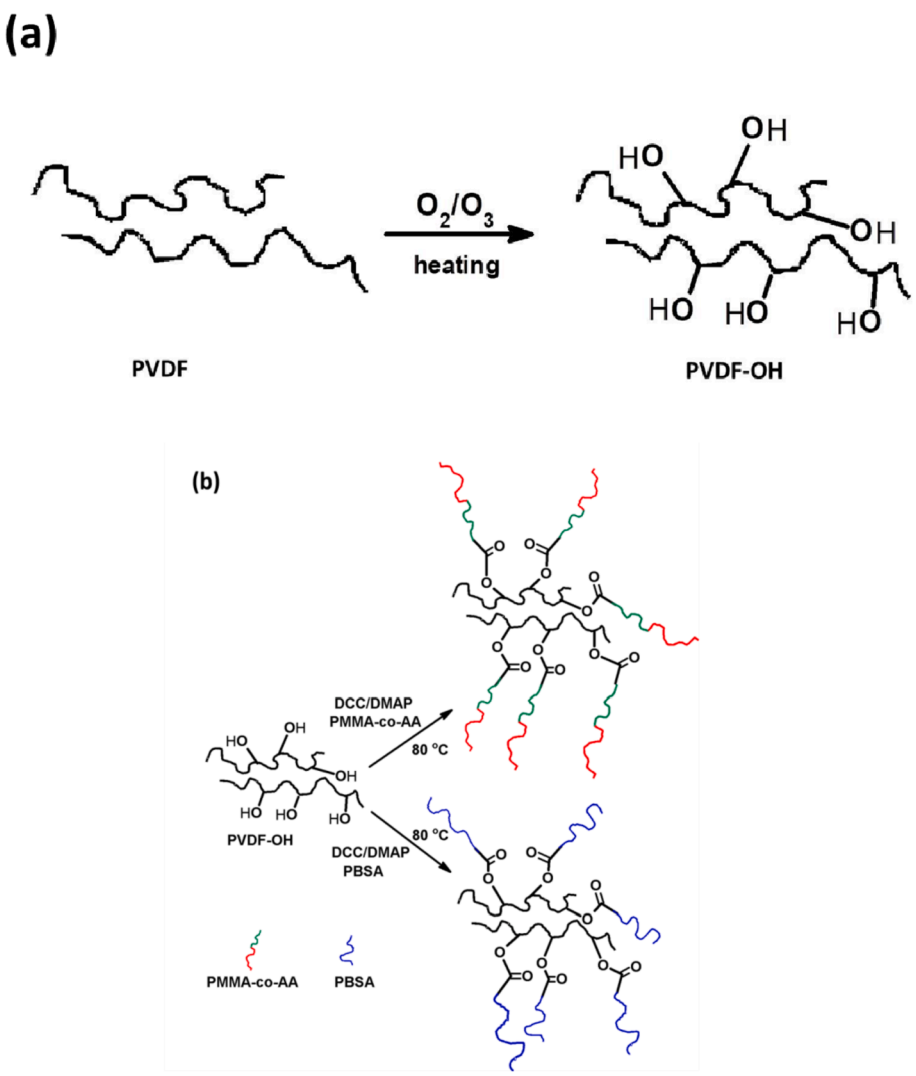

Fig. 1. Schematic representation of the preparation process of (a) ozone treated PVDF and (b) PVDF-g-PMM-co-AA and PVDF-g-PBSA.

in ultrahigh vacuum using a VG-Scientifica (ESCA) X-ray photoelectron spectrophotometer with Al-Ka as X-ray beam source.

The melting temperature (T_m) and percentage of crystallinity of the powder PVDF and its copolymer was measured by differential scanning calorimetry (DSC) using TA analysis (DSC Q2000) under N_2 atmosphere. About 6–8 mg of the sample was taken in a copper pan and heated from room temperature to 220 °C at a heating rate of 10 °C/min and held for 3 min.

Thermogravimetric analysis (TGA) was carried out on a TA instrument mode 2950 in a temperature range of room temperature to 900 °C with a heating rate of 10 °C/min. TGA runs were carried out on samples having a typical weight of 10–20 mg.

For the dielectric measurements, a thin film of 120 μm thickness was prepared by compression molding pressed at 10 bar for 5 min. Alpha-N Analyzer, Novocontrol (Germany) was used to measure the dielectric permittivity and tangent loss in a broad frequency range of $0.01 \leq \omega \leq 10^7$ Hz. Prior to the measurements, the silver paste was used to ensure proper contact.

3. Results and discussion

It is well reported that ozone treated PVDF is an effective means for obtaining suitable functional groups to graft copolymers for various applications [41–43]. The FTIR spectra of powder and ozone treated PVDF, PVDF-g-PMM-co-AA and PVDF-g-PBSA are presented in Fig. 2.

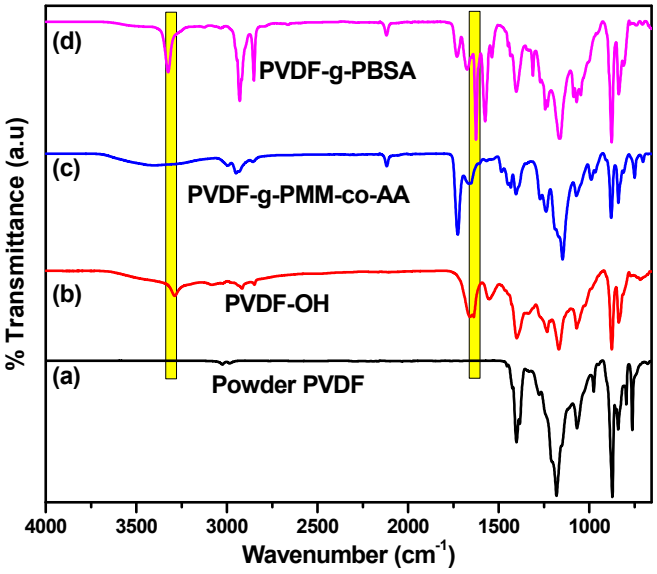

Fig. 2. FTIR spectra of (a) powder PVDF, (b) ozone treated PVDF, (c) PVDF-g-PMM-co-AA and (d) PVDF-g-PBSA.

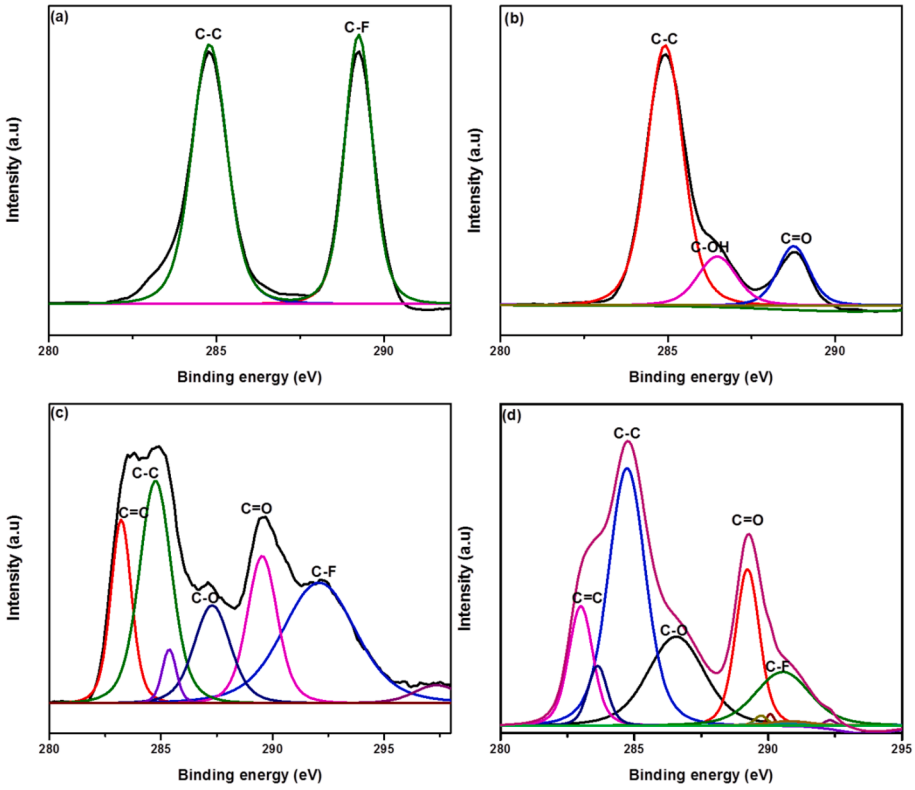

Fig. 3. XPS curve fitted spectra C1s of (a) powder (b) ozone treated PVDF, (c) PVDF-g-PMM-co-AA and (d) PVDF-g-PBSA.

From Fig. 2a and b, it is clearly seen that, as compared to powder PVDF, ozone treated PVDF showed a broad peak at 3295 cm^{-1} (O-H stretching) and 1673 cm^{-1} (carbonyl group C═O) which validates the hydroxylation of PVDF powder to PVDF-OH and this is consistent with previous literature by Liu et al. [44]. The reactive hydroxyl groups present in PVDF-OH allows the introduction of PMM-co-AA and PBSA via hydroxyl-carboxyl reaction. The presence of grafted PMM-co-AA and PBSA on the PVDF surface was also confirmed by FTIR. After grafting with PMM-co-AA and PBSA a strong peak at 1731 cm^{-1} was observed which was attributed to the C-O═C stretching, indicating the successful grafting of PMM-co-AA and PBSA onto PVDF main chain (see Fig. 2c and d). This is due to the esterification reaction of OH group present in PVDF-OH and COOH group of PMM-co-AA and PBSA polymers.

The structural compositions of powder PVDF, PVDF-OH, PVDF-g-PMM-co-AA and PVDF-g-PBSA were also analyzed by XPS. From Fig. 3a, it is clearly seen that for powder PVDF the C 1s core level spectrum can be curve fitted with two major peaks with binding energies of 286 and 290 eV attributed to CH_2 and CF_2 species respectively [45]. On the other hand, ozone treated PVDF (PVDF-OH) can be deconvoluted into three peak components at 284.8 eV, 286.4 eV and 288.67 eV corresponding to C-C, C-OH, and C═O species respectively (Fig. 3b) [62]. The presence of C═O and C-OH indicated that hydroxyl groups have been successfully introduced onto the main chain of PVDF. Liu et al. reported that hydroxylation treatment of PVDF causes the breakage of C-F bonds, resulting in the formation of C-OH [46]. From XPS and FTIR, we can conclude that hydroxyl groups were successfully introduced into the main chain of PVDF.

The synthesized graft copolymers of PVDF was also confirmed by XPS. Fig. 3c shows the C 1s core level spectrum of PVDF-g-PMM-co-AA and can be curve fitted with five peak components having binding energies of 283.3 eV, 284.4 eV, 287.3 eV, 289.4 eV, 290 eV, and 292.2 eV. Among them, the two peaks with binding energy 284.4 eV and 290 eV are attributed to the CH_2 and CF_2 species of PVDF main chain. The other two with binding energies 287.3 eV and 289.4 eV are assigned to the grafted PMM-co-AA corresponding to C-O and C═O. In comparison to PVDF-OH, the peak area of C-C remains the same but after grafting the peak intensity of O-C═C and C═O increased. This could be due to the increased functionalities after grafting, which further confirm the successful grafting of PMM-co-AA chains onto PVDF. Grafting of PBSA on the PVDF surface is presented in Fig. 3d. From Fig. 3d, the C1s peaks can be deconvoluted into five peaks with binding energies at 284.8, 286.7, 289.2, 290.2 and 292 eV corresponds to C-C, C-O and C═O species of the grafted PBSA respectively. The other two peaks are attributed to the PVDF main chain. The XPS results indicate the successful grafting of PMM-co-AA and PBSA onto PVDF which is consistent with FTIR results.

The ^1H NMR spectra of pristine PVDF and ozone treated PVDF are presented in Fig. 4. It is well established that, ^1H NMR of pristine PVDF exhibits two peaks at 3.3 and 2.7 ppm, assigned to the head-to-tail (ht) and head-to-head (hh) bonding arrangements of the vinylidene fluoride units, respectively [47]. In addition to the pristine PVDF peaks, ozone treated PVDF showed new peak at 4–4.5. The peak at 4.5 ppm and 5.8 ppm is due to the proton attached to fluorine and proton attached to hydroxyl group respectively [48]. From FTIR, XPS and NMR, we can conclude that hydroxylation of PVDF powder to PVDF-OH has been successfully takes place after ozonization.

3.1. Effect of grafting on phase transformation

In order to confirm the different crystalline structure in PVDF, FTIR was systematically studied. The vibration bands at 763 cm^{-1} (CF_2 bending and skeletal bending), 795 cm^{-1} (CH_2 rocking), 975 cm^{-1} (CH_2 twisting) are assigned to α-phase while those at 510 cm^{-1} (CF_2 bending), 840 cm^{-1} (CH_2 rocking) represent the β phase [12]. The α phase of PVDF has a unique IR absorption band at 763 cm^{-1}. The presence of exclusively β phase can be observed through the presence of bands at 510 and 840 cm^{-1}. Thus, absorption bands at 763 cm^{-1} and 840 cm^{-1} have been used to evaluate the changes in the fraction of α and β phases in all the samples. From Fig. 5a, powder PVDF displays

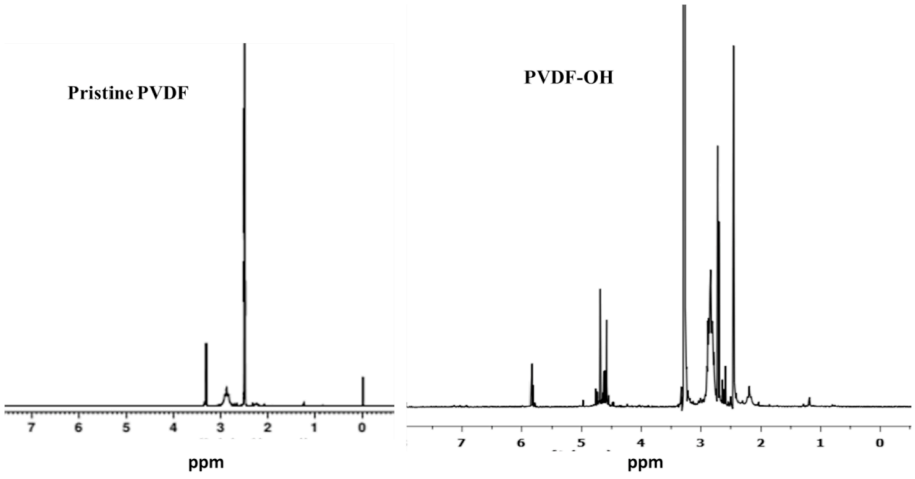

Fig. 4. ^{1}H NMR spectra of pristine PVDF and PVDF-OH.

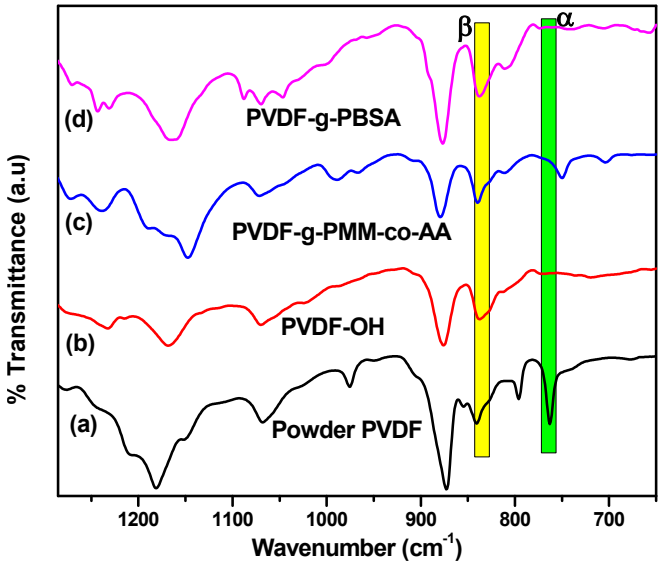

Fig. 5. FTIR spectra of powder and ozone treated PVDF, PVDF-g-PMM-co-AA, and PVDF-g-PBSA.

predominantly α phase (peak at 763 cm^{-1}) with a trace amount of polar β phase (peak at 840 cm^{-1}). After ozonization, the peak intensity at 763 cm^{-1} for the α phase reduces while vibration band at 840 cm^{-1} for the β phase increases (Fig. 5b). In the case of PVDF-g-PMM-co-AA the peak intensity for the β phase significantly improved (Fig. 5c). Interestingly, when grafted with semi-crystalline PBSA (PVDF-g-PBSA), the peak intensity of the α phase was almost completely diminished (Fig. 5d). It confirms that the reaction of PVDF-OH with PBSA facilitates the formation of electroactive β phase in PVDF. It is well known that solution cast neat PVDF also shows predominantly α phase and a trace amount of polar β and γ phases. So grafting of PBSA and PMM-co-AA onto PVDF main chain plays a significant role in the phase transformation from α to β phase. The specific interactions between the –OH groups present in PVDF-OH and –COOH groups present on the grafted polymers assists in the formation of polar β phase in PVDF.

In order to quantify the fraction of β-phase in each sample, IR absorption bands at 763 and 840 cm^{-1} were chosen (characteristic of the α and β phases respectively). Assuming that IR absorption follows the Lambert-Beer law, the A_α and A_β absorbencies, at 763 and 840 cm^{-1}, respectively, can be estimated as,

$$A = \log\frac{I_\alpha^0}{I_\alpha} = K_a\, C{\cdot}X_a\, L \quad (1)$$

$$A_\beta = \log\frac{I_\beta^0}{I_\beta} = K_\beta\, C{\cdot}X_\beta L \quad (2)$$

where, L and C refer to sample thickness and average total monomer concentration, respectively. The incident and transmitted intensity radiations are given by I° and I. The subscripts α and β refer to the two crystalline phases present in the sample. The A_α and A_β values were determined by I° and I at 763 and 840 cm^{-1}, respectively. K is the absorption coefficient while X represents the degree of crystallinity of each phase.

K_α and K_β are the absorption coefficient of the respective bands [45–49] ($K_\alpha = 6.1 \times 10^4$ and $K_\beta = 7.7 \times 10^4$ cm [2]/mol), X_α and X_β are the % crystallinity of the respective phases. The relative β fraction, F (β) was calculated as

$$F(\beta) = \frac{X_\beta}{X_\alpha + X_\beta} = \frac{A_\beta}{(K_\beta/K_\alpha)A_\alpha + A_\beta} = \frac{A_\beta}{(1.26)A_\alpha + A_\beta} \quad (3)$$

It is well reported that the incorporation of surface modified nanoparticles like MWCNTs in PVDF/PMMA blends increases the amount of β phase and enhances the piezoelectric response in PVDF [50]. The effects of functionalization and further grafting with a semi-crystalline PBSA and amorphous PMM-co-AA on the β phase formation in PVDF were investigated systematically. From FTIR, the content of β phases (F (β)) after functionalizing and further grafting are represented in Table 1. From Table 1, β phase increases with functionalizing and grafting. Quantitatively, powder PVDF without any treatment shows a maximum 38% of polar β phase fractions. After ozonization, the amount of β phase was found to be 84%. This enhanced amount of β phase after ozonization could be linked to the presence of –OH and their interaction with PVDF's fluorine atoms. The amount of β phase after grafting with the amorphous PMMA-co-AA (PVDF-g-PMM-co-AA) showed slight enhancement in the β phase. Interestingly, after grafting with crystalline PBSA (PVDF-g-PBSA) the amount of polar β phase

Table 1
Content of polar β phase for untreated, ozone treated PVDF and further grafted with PMM-co-AA and PBSA.

Samples	F(β) content (%)
Powder PVDF	38
PVDF-OH	84
PVDF-g- PMM-co-AA	90
PVDF-g- PBSA	96

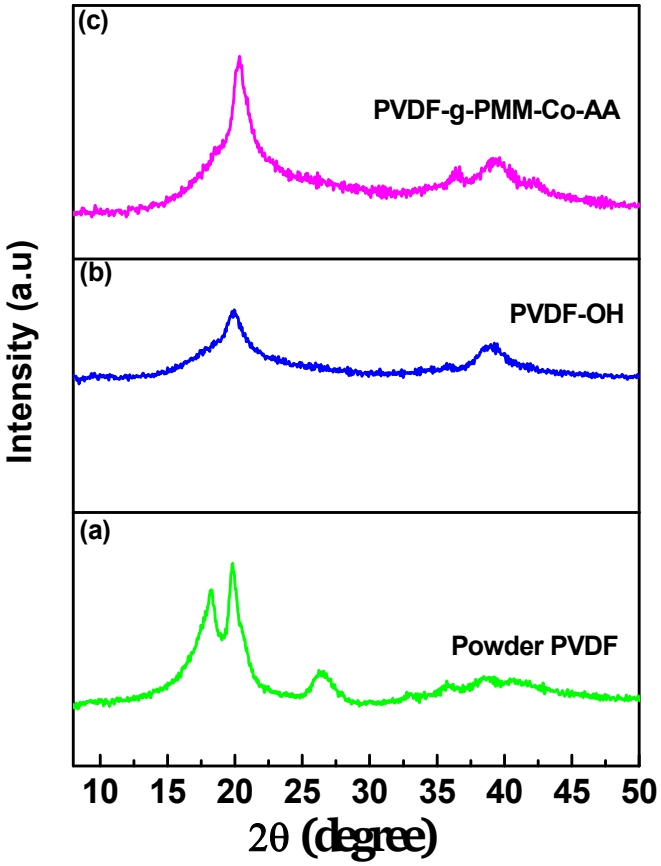

Fig. 6. XRD spectra of powder and ozone treated PVDF, PVDF-g-PMMA–CO–AA.

increased drastically (96%). This enhanced β phase in PVDF-g-PBSA copolymer could be attributed to the specific interaction between –OH groups in PVDF-OH and –COOH groups in PBSA polymer. Manna and Nandi [51] reported that incorporation of ester functionalized MWCNT in PVDF induce 100% electro-active β phase. This was attributed to a specific interaction between the C═O ester group and CF_2 of PVDF group which led to all trans conformation in PVDF. It was also reported that surface groups played an important role in phase transformation in PVDF. For example, incorporation of cellulose in PVDF induces maximum β phase as compared to CNT and clay nanoparticles [52]. This is due to the specific interaction between –OH group present in cellulose and fluorine in PVDF. From FTIR, we can conclude that the grafting of PBSA onto PVDF is more effective to induce polar β phase.

The presence of different crystalline polymorphism was further examined by XRD. Fig. 6 illustrates XRD patterns of powder PVDF, PVDF-OH, PVDF-g-PMM-co-AA and PVDF-g-PBSA. The characteristic peaks at 18.4°, 20°, and 26.2° were ascribed to the diffraction peaks (020), (110) and (021) of α phase and peak at 20.4° was ascribed to diffraction peak (200) for the polar β phase [53]. Fig. 5a depicted that, powder PVDF without any functionalization exhibit major crystalline peaks at 2θ = 17.8°, 18.4° and 19.9° which are assigned to the crystalline structure of the α phase. In contrast, after ozonization and grafting, all the α peaks were absent and a new and single peak at 2θ = 20.4°, assigned for the β phase, appears (Fig. 6b, c, and d). Thus strong covalent interaction can induce the formation of only polar β in PVDF. This covalent interaction restricts molecular mobility of PVDF chains and results in all trans (TTT) conformation echoes with the FTIR results. From FTIR and XRD, it is well evident that functionalized PVDF itself showed β polymorph, which to some extent, can be further enhanced by grafting amorphous or crystalline polymers.

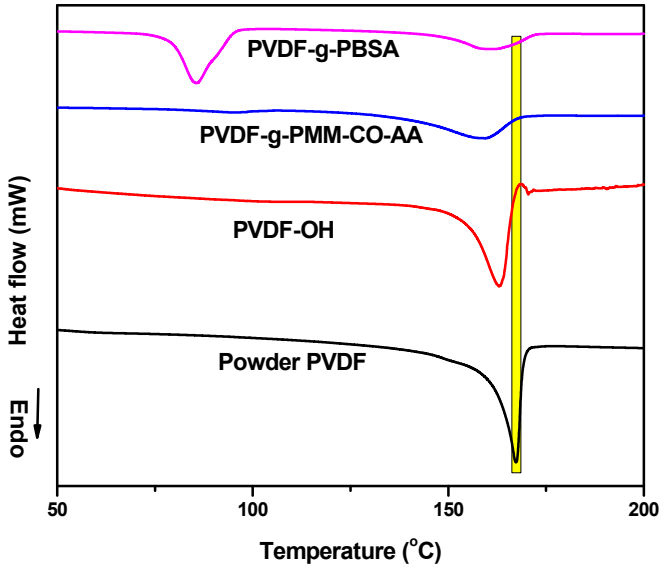

Fig. 7. DSC thermograms for powder PVDF, PVDF-OH, PVDF-g-PMM-co-AA, and PVDF-g-PBSA at a heating rate of 10 °C/min.

3.2. Crystalline morphology: effect of grafting

The effects of ozonization and further grafting of amorphous PMM-co-AA and semi-crystalline PBSA on PVDF on the crystalline morphology were analyzed by DSC. The DSC thermograms of powder PVDF, PVDF-OH, PVDF-g-PMM-co-AA and PVDF-g-PBSA are illustrated in Fig. 7. From Fig. 7, the melting temperature for powder and ozone treated PVDF has been found to be 167 °C and 165 °C, respectively. This shows ozonization does not significantly change the melting temperature of PVDF. But after grafting amorphous PMM-co-AA polymer, a new transition at 96 °C was observed, which is assigned to the glass transition temperature of PMM-co-AA. The existence of both Tg of the PMM-co-AA graft and T_m of PVDF indicates successful grafting of PMM-co-AA onto PVDF main chain. In the case of grafting semi-crystalline PBSA onto PVDF (PVDF-g-PBSA) bimodal melting peaks at 85 °C and 161 °C was observed. The existence of two melting points may be related to the presence of PBSA and PVDF. The grafting of polymers on PVDF showed depression in melting point, as referred [54].

From the melting endotherms % crystallinity was calculated by the following equation

$$\Delta X_c = \frac{\Delta H_m}{\Delta H_{100}} \quad (4)$$

where ΔH_m is the melting enthalpy of the sample and ΔH_{100} is the melting enthalpy for a 100% crystalline sample (ΔH_{100} = 104.50 J/g for PVDF) [55]. From Table 2, the percentage of crystallinity (% X_C) for powder and ozone treated PVDF has been found to be 37 and 34. This showed that there is no significant change in percent crystallinity after ozonization. After grafting with PMM-co-AA and PBSA the % crystallinity decreases (Table 2). It is reported that the addition of amorphous polymers decreases the percent of crystallinity because it acts as a diluent. Qiu et al. investigated the crystalline morphology of PVDF/PBSA

Table 2
% Crystallinity measured by DSC for powder PVDF, PVDF-OH and PVDF-g-PMM-co-AA.

Samples	% crystallinity (X_c)
Powder PVDF	36
PVDF-OH	34
PVDF-g-PMM-co-AA	28
PVDF-g-PBSA	30

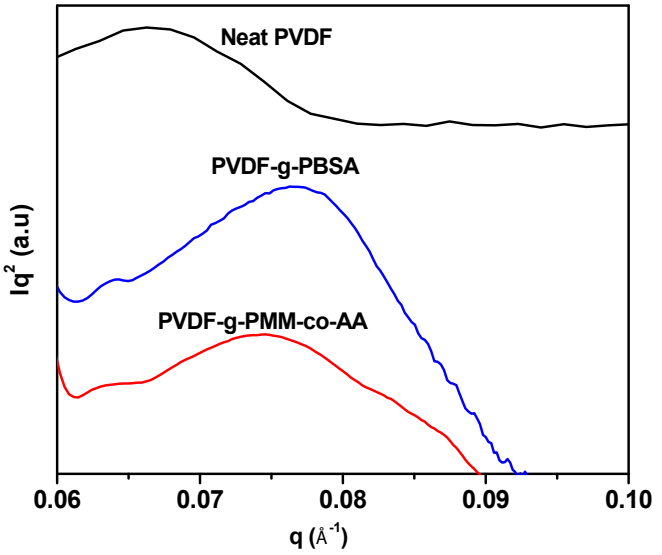

Fig. 8. 1D SAXS (Lorenz corrected) plots for neat PVDF, PVDF-g-PMM-co-AA and PVDF-g-PBSA at room temperature.

Table 3
Comparison of long period (L_w), crystalline lamellae (L_C) and amorphous layer (L_a) thicknesses of neat PVDF, PVDF-OH, PVDF-g-PMM-co-AA and PVDF-g-PBSA at room temperature.

	L_w(Å)	L_C (Å)	L_a (Å)
Neat PVDF	94	40	54
PVDF-OH	89	30	59
PVDF-g-PMM-co-AA	85	24	61
PVDF-g-PBSA	82	25	57

blends [56]. The melting temperature of PVDF decreases with increasing concentration of PBSA.

In order to obtain a deep insight into the lamellar morphology and orientation of PVDF crystallites, small angle x-ray scattering (SAXS) was carried out. Fig. 8 shows the SAXS (Iq [2] versus q) plots of neat PVDF, PVDF-OH, PVDF-g-PMM-co-AA, and PVDF-g-PBSA and the results are summarized in Table 3. The q peak position is related to the value of the long period (L_w), corresponding to the thickness of crystalline lamellae (L_c) and amorphous regions (L_a) and can be calculated by the Bragg equation: $L_w = \frac{2\pi}{q_{max}}$

From Table 3, the values of both long period (L_w) and crystalline lamellae (L_c) decrease in PVDF-OH as compared to neat PVDF. This decrease in a long period (L_w) and crystalline lamellae (L_c) is more significant in the case of PVDF-g-PMM-co-AA and PVDF-g-PBSA. As discussed earlier, from FTIR and XRD results in the neat PVDF exhibited predominantly α-phase and PVDF-g-PMM-co-AA and PVDF-g-PBSA predominantly β-phase. The decrease in a long period and crystalline lamellae in PVDF-g-PMM-co-AA and PVDF-g-PBSA samples could be due to the presence of β-crystal. This is consistent with available literature [57].

In order to evaluate the thermal stability of grafted PVDF thermogravimetric analysis (TGA) of Powder PVDF, PVDF-OH, PVDF-g-PMM-co-AA, and PVDF-g-PBSA were carried out. Fig. 9a depicts that for powder PVDF, a single degradation temperature was observed and a weight loss at a temperature range of 430 °C–500 °C. This was attributed to the degradation of PVDF chain. The ozone treated PVDF (PVDF-OH) also showed a single step degradation temperature (410 °C). The degradation temperature of ozone-treated PVDF (PVDF-OH) was slightly lower than that of powder PVDF (Fig. 9b). Both powder and ozone treated PVDF showed outstanding temperature stability. The PVDF-g-PMM-co-AA showed four steps degradation at 203 °C, 270 °C, 325 °C and 420 °C (Fig. 9c). From 203 to 323 °C can be attributed to the grafted PMM-co-AA and 420 °C to the backbone respectively. For PVDF-g-PBSA the temperature of three-step degradation was observed at 236 °C, 325 °C and 420 °C (Fig. 9d). The first step, from 236 to 325 °C can be attributed to the grafted PBSA functional groups and 420 °C to the PVDF main chain respectively.

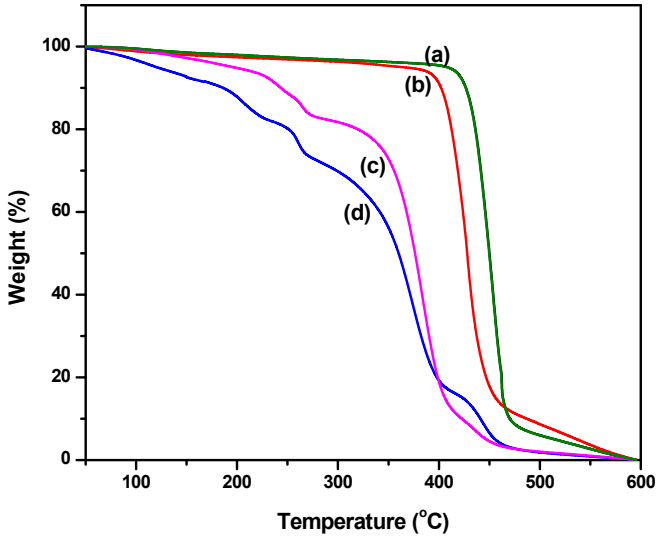

Fig. 9. Thermogravimetric analysis of (a) powder PVDF, (b) PVDF-OH, (c) PVDF-g-PMM-co-AA and (d) PVDF-g-PBSA.

3.3. Dielectric properties and piezoelectric effect of grafting

It was well reported that functionalization of PP with –OH (PP-OH) increases the dielectric properties [58]. This is due to the polar –OH group creates polarization centers in PP. The dielectric properties of PVDF depend on the amount of polar β phase. Samples with higher β phase showed higher dielectric values. The incorporation of –OH and $–NH_2$ functionalities into PVDF main chain enhances the dielectric properties of PVDF. The dielectric properties of thin films of neat PVDF, PVDF-OH, PVDF-g-PMM-co-AA, and PVDF-g-PBSA as a function of frequency at room temperature were investigated. As shown in Fig. 10a, the dielectric permittivity increases after functionalization and further grafting. For neat PVDF, the dielectric permittivity was found to be around 7, but after ozonization, it increased to 10. This enhanced dielectric properties after ozonization could be attributed to the higher dipole and higher polarizability of the –OH group attached to the PVDF surface. After grafting with PMM-co-AA (PVDF-g-PMM-co-AA) the dielectric property has been found to be increased to 11. More interestingly after grafting with PBSA (PVDF-g-PBSA), the dielectric behavior increases to 12. This could be due to a higher amount of electroactive β as compared to the other samples as revealed from FTIR. The change in loss tangent of neat PVDF, PVDF-OH, PVDF-g-PMM-co-AA and PVDF-g-PBSA samples measured at room temperature are presented in Fig. 10b. For PVDF-OH, PVDF-g-PMM-co-AA, and PVDF-g-PBSA, a decrease in the loss tangent was observed as compared to neat PVDF. PVDF-OH, PVDF-g-PMM-co-AA, and PVDF-g-PBSA predominantly composed of β-phase which has higher packing density and polarity and this leads to lower molecular mobility and thus the loss tangent decreases or it could be due to their low crystallinity of PVDF-g-PMM-co-AA and PVDF-g-PBSA as revealed from DSC.

It is well known that the piezoelectric coefficient in PVDF depends on the amount and orientation of polar β phase. Samples with higher β phase and higher orientation showed higher piezoelectric coefficient. The piezoelectric coefficients (d_{33}) of powder PVDF, PVDF-OH, PVDF-g-PMM-co-AA, and PVDF-g-PBSA were compared. From FTIR, we have established that grafting PBSA on PVDF results in the maximum amount

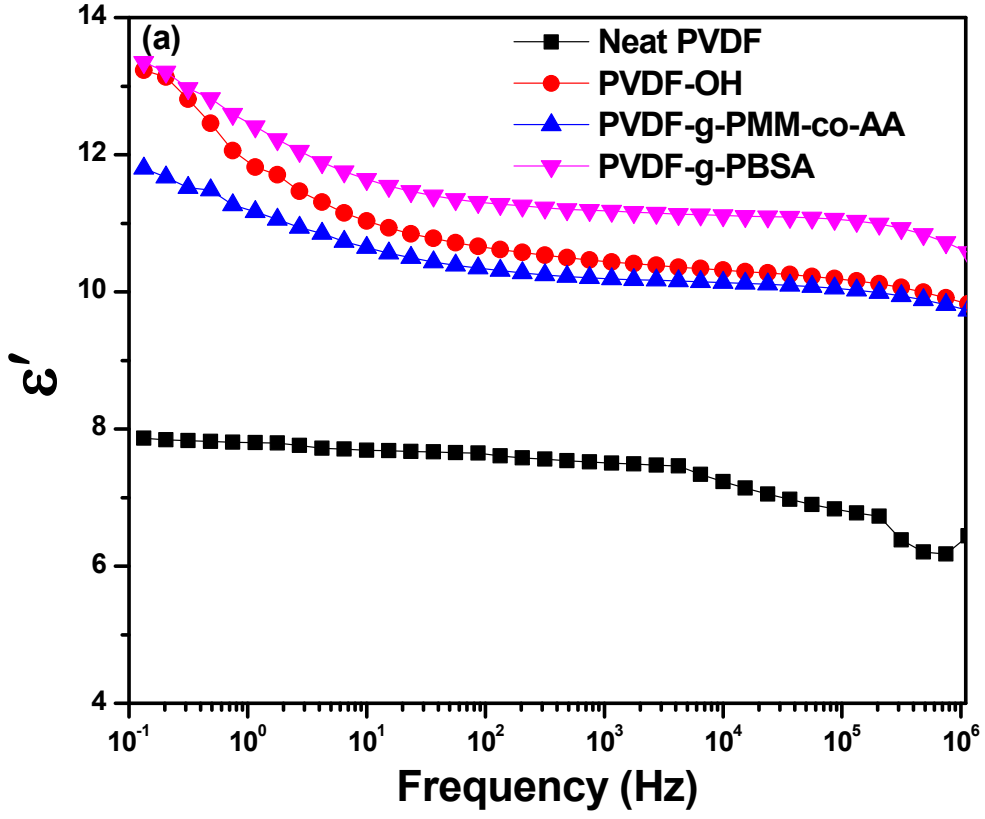

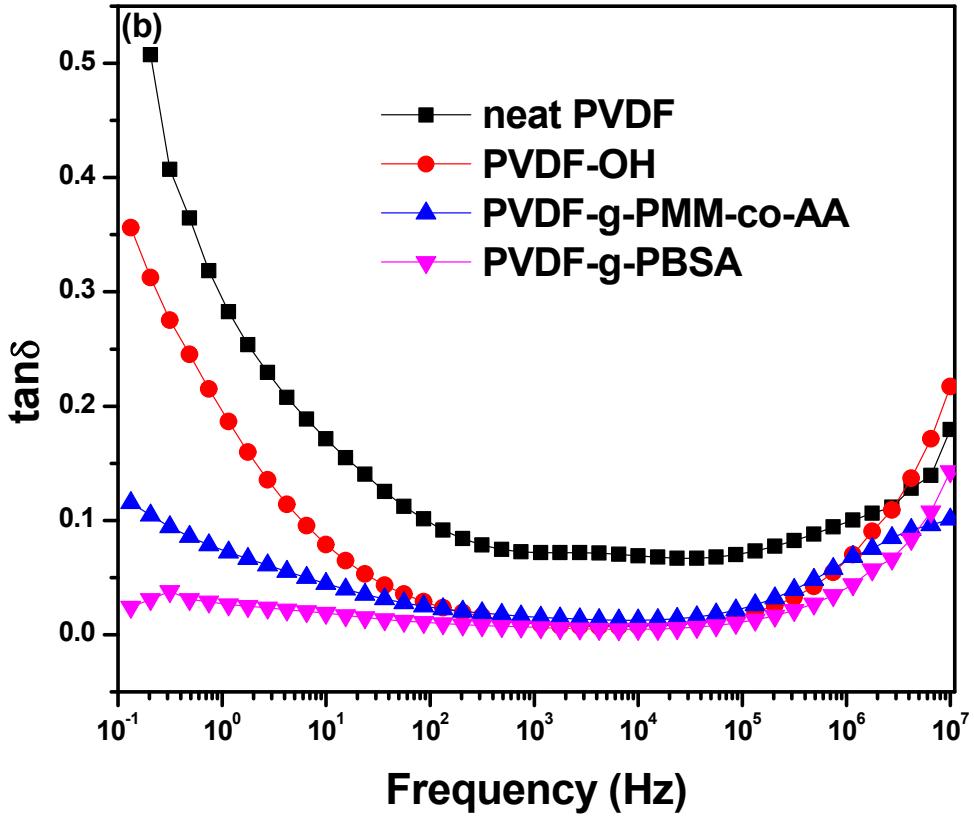

(caption on next page)

Fig. 10. Variation in (a) dielectric permittivity and (b) loss tangent with frequency for neat PVDF, PVDF-OH, PVDF-g-PMM-co-AA, and PVDF-g-PBSA at room temperature.

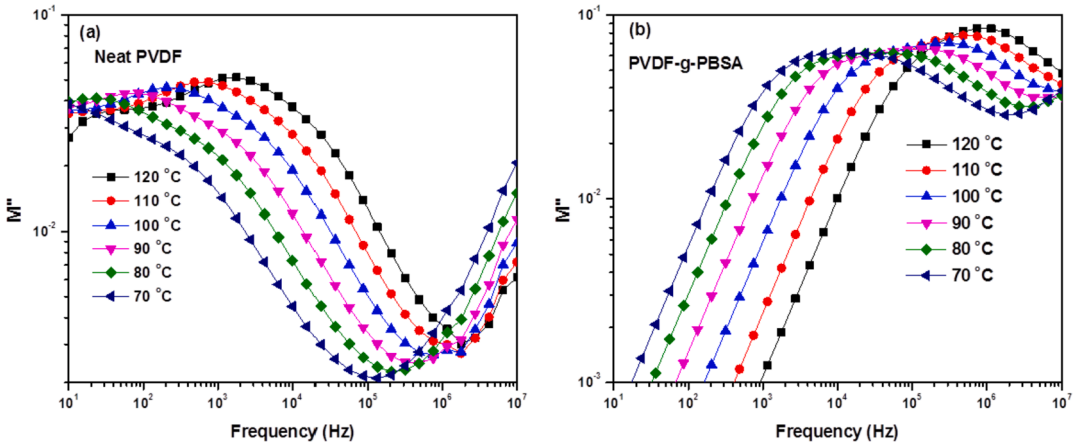

Fig. 11. Dielectric loss modulus (M″) as a function of frequency at different temperature for (a) pressed neat PVDF, (b) PVDF-g-PBSA samples.

of β phase in PVDF. It is quite reasonable to expect a higher piezoelectric coefficient for samples with higher amount of β phase. PVDF-OH and PVDF-g-PMM-co-AA exhibited d_{33} values of −7 pC/N as they have the same amount of β phase. Interestingly, the maximum d_{33} value of −17 pC/N was obtained for PVDF-g-PBSA thin films. This is due to the higher amount of β phase induced in PVDF upon grafting with PBSA. A similar observation was available in the literature. Enhanced amount of polar β phase and piezoelectric coefficient after stretching in PVDF nanohybrids were reported. This was explained by samples with higher polar β-phase led to enhanced d_{33} values [59].

3.4. Dielectric and structural relaxations

We are interested in investigating the dielectric relaxation of α- and β-phases of neat PVDF, PVDF-OH, PVDF-g-PMM-co-AA, and PVDF-g-PBSA. From FTIR and XRD, PVDF-g-PMM-co-AA and PVDF-g-PBSA exhibited maximum β-phase and neat PVDF showed predominantly α-phase. The frequency dependence of dielectric loss modulus (M″) for neat PVDF, PVDF-OH, PVDF-g-PMM-co-AA, and PVDF-g-PBSA at different temperatures are presented in Fig. 10. It is well reported that PVDF shows three relaxations namely, α_a, α_c and β corresponding to segmental motion in the crystalline-amorphous interphase, an imperfection in the crystalline phase and local motion, respectively [60]. The dielectric relaxation peak shifts to a higher frequency with the temperature that corresponds to the increase in chain mobility with temperature. Fig. 11a shows the dielectric loss modulus (M″) of as pressed neat PVDF as a function of frequency at different temperatures. It is evident from Fig. 11a that neat PVDF exhibited only α_c relaxation in the measured frequency window which shifts to a higher frequency as the temperature increases. This is consistent with the available literature [61]. For PVDF-OH and PVDF-g-PMM-co-AA samples also showed a single relaxation and shifted to a higher frequency (not shown here). For PVDF-g-PBSA, the dielectric relaxation intensity was shifted to a higher frequency (Fig. 11b). It was reported that for PVDF samples composed of predominantly β-phase, the dielectric relaxation shifted to a higher frequency with an increase in temperature. The explanation for the shift to higher frequency is due to the formation of predominantly polar β-phase in PVDF-OH, PVDF-g-PMM-co-AA and PVDF-g-PBSA samples. These β crystals are considered as defect crystals and less time is required to orient these crystals.

4. Conclusions

In this study, PVDF-OH has been prepared via ozonization to graft PMM-co-AA and PBSA to design PVDF copolymers. The –OH groups on PVDF-OH react with –COOH group present in PMM-co-AA and PBSA to form an ester. The effects of functionalization and further grafting on the polar β phase formation and piezoelectric coefficient in PVDF have been investigated. The presence of –OH group in the ozone-treated PVDF was confirmed by FTIR and XPS. FTIR and XRD results show that both functionalization and grafting enhance the electro-active β phase crystals while reducing the growth of α phase crystals as compared to the untreated PVDF. Quantitatively, the extent of polar β phase has been enhanced from 38% for untreated PVDF to 84% after ozonization. Interestingly, the enhancement is more pronounced after grafting. More interestingly, after grafting PBSA onto PVDF almost complete transformation from α to β phase (96%) was observed. This is attributed to the specific covalent interaction between the –OH group present in PVDF-OH and –COOH groups of PBSA that led to ester formation. This strong covalent interaction helps to align the PVDF chains in trans conformation and thus more β phase crystals are formed. The remarkably enhanced β phase was reflected in higher dielectric constant and piezoelectric coefficient (d_{33}) as compared to untreated PVDF. The PVDF-g-PBSA copolymer showed higher piezoelectric and dielectric constant with low dielectric loss as compared to untreated PVDF. In summary, this study provides a simple method to prepare covalently grafted PMM-co-AA and PBSA onto PVDF with enhanced polar β phase, dielectric constant and piezoelectric coefficient.

Acknowledgments

Giridhar Madras thanks Department of Science and Technology (DST), India for the J.C. Bose fellowship. Authors would also like to acknowledge the MNCF facilities at CeNSE at IISc.

References

[1] Z.M. Dang, J.K. Yuan, S.H. Yao, R.J. Liao, Flexible nanodielectric materials with high permittivity for power energy storage, Adv. Mater. 25 (2013) 6334–6365.
[2] M. Arbatti, X.B. Shan, Z.Y. Cheng, Ceramic-polymer composites with high dielectric constant, Adv. Mater. 19 (2007) 1369.
[3] L. Lebrun, D. Guyomar, B. Guiffard, P.J. Cottinet, C. Putson, The Characterisation of the harvesting capabilities of an electrostrictive polymer composite, Sens. Actuators A Phys. 153 (2009) 251–257.
[4] H. Ohigashi, Electromechanical properties of polarized polyvinylidene fluoride films as studied by the piezoelectric resonance method, J. Appl. Phys. 47 (1976) 949–955.

[5] A.V. Shirinov, W.K. Schomburg, Pressure sensor from a PVDF film, Sens. Actuators A Phys. 142 (2008) 48–55.
[6] H. Kawai, The piezoelectricity of poly (vinylidene fluoride), Jpn. J. Appl. Phys. 8 (1969) 975.
[7] M. Broadhurst, G. Davis, J. McKinney, R. Collins, Piezoelectricity and pyroelectricity in polyvinylidene fluoride—a model, J. Appl. Phys. 49 (1978) 4992–4997.
[8] Y. Wada, R. Hayakawa, Piezoelectricity and pyroelectricity of polymers, Jpn. J. Appl. Phys. 15 (1976) 2041.
[9] C. Purvis, P. Taylor, Piezoelectricity and pyroelectricity in polyvinylidene fluoride: influence of the lattice structure, J. Appl. Phys. 54 (1983) 1021–1028.
[10] M. Sharma, G. Madras, S. Bose, Process induced electroactive β-polymorph in PVDF: effect on dielectric and ferroelectric properties, Phys. Chem. Chem. Phys. 16 (2014) 14792–14799.
[11] V. Sencadas, R. Gregorio Jr., S. Lanceros-Méndez, α to β phase transformation and microestructural changes of PVDF films induced by uniaxial stretch, J. Macromol. Sci. 48 (2009) 514–525.
[12] A. Salimi, A. Yousefi, Analysis method: FTIR studies of β-phase crystal formation in stretched PVDF films, Polym. Test. 22 (2003) 699–704.
[13] A. Gebrekrstos, M. Sharma, G. Madras, S. Bose, New physical insights into shear history dependent polymorphism in poly(vinylidene fluoride), Cryst. Growth Des. 16 (2016) 2937–2944.
[14] D. Yang, Y. Chen, β-phase formation of poly (vinylidene fluoride) from the melt induced by quenching, J. Mater. Sci. Lett. 6 (1987) 599–603.
[15] A.A. Yousefi, Influence of Polymer Blending on Crystalline Structure of Polyvinylidene Fluoride, (2011).
[16] R. Gregorio Jr., N.C.P. de Souza Nociti, Effect of PMMA addition on the solution crystallization of the alpha and beta phases of poly (vinylidene fluoride)(PVDF), J. Phys. D Appl. Phys. 28 (1995) 432.
[17] P. Martins, C. Caparros, R. Gonçalves, P.M. Martins, M. Benelmekki, G. Botelho, S. Lanceros-Mendez, Role of nanoparticle surface charge on the nucleation of the electroactive β-Poly(vinylidene fluoride) nanocomposites for sensor and actuator applications, J. Phys. Chem. C 116 (2012) 15790–15794.
[18] S. Manna, A.K. Nandi, Piezoelectric β polymorph in poly (vinylidene fluoride)-functionalized multiwalled carbon nanotube nanocomposite films, J. Phys. Chem. C 111 (2007) 14670–14680.
[19] M. Ataur Rahman, G.-S. Chung, Synthesis of PVDF-graphene nanocomposites and their properties, J. Alloy. Comp. 581 (2013) 724–730.
[20] P. Costa, J. Silva, V. Sencadas, C.M. Costa, F. Van Hattum, J.G. Rocha, S. Lanceros-Méndez, The effect of fibre concentration on the α to β-phase transformation, degree of crystallinity and electrical properties of vapour grown carbon nanofibre/poly (vinylidene fluoride) composites, Carbon 47 (2009) 2590–2599.
[21] X. Huang, P. Jiang, C. Kim, F. Liu, Y. Yin, Influence of aspect ratio of carbon nanotubes on crystalline phases and dielectric properties of poly(vinylidene fluoride), Eur. Polym. J. 45 (2009) 377–386.
[22] S. Yu, W. Zheng, W. Yu, Y. Zhang, Q. Jiang, Z. Zhao, Formation mechanism of β-phase in PVDF/CNT composite prepared by the sonication method, Macromolecules 42 (2009) 8870–8874.
[23] F. He, S. Lau, H.L. Chan, J. Fan, High dielectric permittivity and low percolation threshold in nanocomposites based on poly (vinylidene fluoride) and exfoliated graphite nanoplates, Adv. Mater. 21 (2009) 710–715.
[24] M. El Achaby, F. Arrakhiz, S. Vaudreuil, E. Essassi, A. Qaiss, Piezoelectric β-polymorph formation and properties enhancement in graphene oxide–PVDF nanocomposite films, Appl. Surf. Sci. 258 (2012) 7668–7677.
[25] R.K. Layek, S. Samanta, D.P. Chatterjee, A.K. Nandi, Physical and mechanical properties of poly (methyl methacrylate)-functionalized graphene/poly (vinylidine fluoride) nanocomposites: piezoelectric β polymorph formation, Polymer 51 (2010) 5846–5856.
[26] L.-g. Wu, X.-y. Zhang, T. Wang, C.-h. Du, C.-h. Yang, Enhanced performance of polyvinylidene fluoride ultrafiltration membranes by incorporating TiO2/graphene oxide, Chem. Eng. Res. Des. 141 (2019) 492–501.
[27] S. Song, Z. Zheng, Y. Bi, X. Lv, S. Sun, Improving the electroactive phase, thermal and dielectric properties of PVDF/graphene oxide composites by using methyl methacrylate-co-glycidyl methacrylate copolymers as compatibilizer, J. Mater. Sci. 54 (2019) 3832–3846.
[28] A. Gebrekrstos, G. Madras, S. Bose, Piezoelectric response in electrospun poly(vinylidene fluoride) fibers containing fluoro-doped graphene derivatives, ACS Omega 3 (2018) 5317–5326.
[29] B. Mohammadi, A.A. Yousefi, S.M. Bellah, Effect of tensile strain rate and elongation on crystalline structure and piezoelectric properties of PVDF thin films, Polym. Test. 26 (2007) 42–50.
[30] J. Gomes, J.S. Nunes, V. Sencadas, S. Lanceros-Méndez, Influence of the β-phase content and degree of crystallinity on the piezo-and ferroelectric properties of poly (vinylidene fluoride), Smart Mater. Struct. 19 (2010) 065010.
[31] T. Kaura, R. Nath, M. Perlman, Simultaneous stretching and corona poling of PVDF films, J. Phys. D Appl. Phys. 24 (1991) 1848.
[32] V. Tomer, E. Manias, C.A. Randall, High field properties and energy storage in nanocomposite dielectrics of poly(vinylidene fluoride-hexafluoropropylene), J. Appl. Phys. 110 (2011).
[33] Y. Shen, D. Shen, X. Zhang, J. Jiang, Z. Dan, Y. Song, Y. Lin, M. Li, C.-W. Nan, High energy density of polymer nanocomposites at a low electric field induced by modulation of their topological-structure, J. Mater. Chem. 4 (2016) 8359–8365.
[34] B. Chu, X. Zhou, K. Ren, B. Neese, M. Lin, Q. Wang, F. Bauer, Q. Zhang, A dielectric polymer with high electric energy density and fast discharge speed, Science 313 (2006) 334–336.
[35] F. He, S. Lau, H.L. Chan, J.T. Fan, High dielectric permittivity and low percolation threshold in nanocomposites based on poly(vinylidene fluoride) and exfoliated graphite nanoplates, Adv. Mater. 21 (2009) 710-+.
[36] G. Zhai, S. Toh, W. Tan, E. Kang, K. Neoh, C. Huang, D. Liaw, Poly (vinylidene fluoride) with grafted zwitterionic polymer side chains for electrolyte-responsive microfiltration membranes, Langmuir 19 (2003) 7030–7037.
[37] Y. Chang, W.-J. Chang, Y.-J. Shih, T.-C. Wei, G.-H. Hsiue, Zwitterionic sulfobetaine-grafted poly (vinylidene fluoride) membrane with highly effective blood compatibility via atmospheric plasma-induced surface copolymerization, ACS Appl. Mater. Interfaces 3 (2011) 1228–1237.
[38] S. Holmberg, T. Lehtinen, J. Näsman, D. Ostrovskii, M. Paronen, R. Serimaa, F. Sundholm, G. Sundholm, L. Torell, M. Torkkeli, Structure and properties of sulfonated poly [(vinylidene fluoride)–g-styrene] norous membranes porous membranes, J. Mater. Chem. 6 (1996) 1309–1317.
[39] L. Ying, P. Wang, E. Kang, K. Neoh, Synthesis and characterization of poly (acrylic acid)-graft-poly (vinylidene fluoride) copolymers and pH-sensitive membranes, Macromolecules 35 (2002) 673–679.
[40] L. Dong, X. Liu, Z. Xiong, D. Sheng, Y. Zhou, C. Lin, Y. Yang, Design of UV-absorbing PVDF membrane via surface-initiated AGET ATRP, Appl. Surf. Sci. 435 (2018) 680–686.
[41] P. Wang, K. Tan, E. Kang, K. Neoh, Synthesis, characterization and anti-fouling-properties of poly (ethylene glycol) grafted poly (vinylidenefluoride) copolymer membranes, J. Mater. Chem. 11 (2001) 783–789.
[42] Y. Chang, Y.-J. Shih, R.-C. Ruaan, A. Higuchi, W.-Y. Chen, J.-Y. Lai, Preparation of poly (vinylidene fluoride) microfiltration membrane with uniform surface-copolymerized poly (ethylene glycol) methacrylate and improvement of blood compatibility, J. Membr. Sci. 309 (2008) 165–174.
[43] Y. Chang, C.-Y. Ko, Y.-J. Shih, D. Quémener, A. Deratani, T.-C. Wei, D.-M. Wang, J.-Y. Lai, Surface grafting control of PEGylated poly (vinylidene fluoride) antifouling membrane via surface-initiated radical graft copolymerization, J. Membr. Sci. 345 (2009) 160–169.
[44] Y. Liu, J. Lee, E. Kang, P. Wang, K. Tan, Synthesis, characterization and electrochemical transport properties of the poly (ethyleneglycol)–grafted poly (vinylidenefluoride) nanoporous membranes, React. Funct. Polym. 47 (2001) 201–213.
[45] J.F. Moulder, Handbook of X-ray photoelectron spectroscopy, Phys. Electron. (1995) 230–232.
[46] D. Liu, Y. Chen, N. Zhang, X. He, Controlled grafting of polymer brushes on poly (vinylidene fluoride) films by surface-initiated atom transfer radical polymerization, J. Appl. Polym. Sci. 101 (2006) 3704–3712.
[47] M. Tao, F. Liu, L. Xue, Hydrophilic poly (vinylidene fluoride)(PVDF) membrane by in situ polymerisation of 2-hydroxyethyl methacrylate (HEMA) and micro-phase separation, J. Mater. Chem. 22 (2012) 9131–9137.
[48] L.D.S. Yadav, Organic Spectroscopy, Springer Science & Business Media, 2013.
[49] J.R. Gregorio, M. Cestari, Effect of crystallization temperature on the crystalline phase content and morphology of poly(vinylidene fluoride), J. Polym. Sci., Part B: Polym. Phys. 32 (1994) 859–870.
[50] M. Sharma, K. Sharma, S. Bose, Segmental relaxations and crystallization-induced phase separation in PVDF/PMMA blends in the presence of surface-functionalized multiwall carbon nanotubes, J. Phys. Chem. B 117 (2013) 8589–8602.
[51] S. Manna, A.K. Nandi, Piezoelectric β polymorph in poly(vinylidene fluoride)-functionalized multiwalled carbon nanotube nanocomposite films, J. Phys. Chem. C 111 (2007) 14670–14680.
[52] S. Bodkhe, P. Rajesh, S. Kamle, V. Verma, Beta-phase enhancement in polyvinylidene fluoride through filler addition: comparing cellulose with carbon nanotubes and clay, J. Polym. Res. 21 (2014) 434.
[53] R. Gregorio Jr., Determination of the α, β, and γ crystalline phases of poly (vinylidene fluoride) films prepared at different conditions, J. Appl. Polym. Sci. 100 (2006) 3272–3279.
[54] J.F. Hester, P. Banerjee, Y.Y. Won, A. Akthakul, M.H. Acar, A.M. Mayes, ATRP of amphiphilic graft copolymers based on PVDF and their use as membrane additives, Macromolecules 35 (2002) 7652–7661.
[55] K. Nakagawa, Y. Ishida, Annealing effects in poly (vinylidene fluoride) as revealed by specific volume measurements, differential scanning calorimetry, and electron microscopy, J. Polym. Sci. Polym. Phys. Ed 11 (1973) 2153–2171.
[56] Z. Qiu, C. Yan, J. Lu, W. Yang, Miscible crystalline/crystalline polymer blends of poly (vinylidene fluoride) and poly (butylene succinate-co-butylene adipate): spherulitic morphologies and crystallization kinetics, Macromolecules 40 (2007) 5047–5053.
[57] M. Sharma, G. Madras, S. Bose, Cooperativity and structural relaxations in PVDF/PMMA blends in the presence of MWNTs: an assessment through SAXS and dielectric spectroscopy, Macromolecules 47 (2014) 1392–1402.
[58] T.M. Chung, Functionalization of polypropylene with high dielectric properties: applications in electric energy storage, Green Sustain. Chem. 2 (2012) 29.
[59] V.K. Tiwari, A.K. Prasad, V. Singh, K.K. Jana, M. Misra, C.D. Prasad, P. Maiti, Nanoparticle and process induced super toughened piezoelectric hybrid materials: the effect of stretching on filled system, Macromolecules 46 (2013) 5595–5603.
[60] J.W. Sy, J. Mijovic, Reorientational dynamics of poly(vinylidene fluoride)/Poly (methyl methacrylate) blends by broad-band dielectric relaxation spectroscopy, Macromolecules 33 (2000) 933–946.
[61] M. Sharma, G. Madras, S. Bose, Unusual fragility and cooperativity in glass-forming and crystalline PVDF/PMMA blends in the presence of multiwall carbon nanotubes, Macromolecules 48 (2015) 2740–2750.
[62] P.K. Samantaray, et al., PVDF/PBSA membranes with strongly coupled phosphonium derivatives and graphene oxide on the surface towards antibacterial and antifouling activities, J. Membr. Sci. (2018), https://doi.org/10.1016/j.memsci.2017.11.